Dielectric permittivity measurements on highly conductive perfluoropolyether microemulsions at frequencies up to 100 MHz

Meas. Sci. Technol. 4 (1993) 627–631. Printed in the UK

Dielectric permittivity measurements on highly conductive perfluoropolyether microemulsions at frequencies up to 100 MHz

M Grazia Giri†, Marcello Carlà†, Cecilia M C Gambi†, Donatella Senatra†, A Chittofrati‡ and A Sanguineti‡

† Department of Physics, University of Florence, L E Fermi 2, 50125 Firenze, Italy
‡ Ausimont, R&D Centre, Colloid Laboratory, V S Pietro 50, 20021 Bollate (Milano), Italy

Received 7 February 1992, in final form 12 November 1992, accepted for publication 15 January 1993

Abstract. The impedance analysis technique has been used to measure the complex permittivity and conductivity of highly conductive perfluoropolyether microemulsions. The cell construction details, calibration procedure and data analysis procedure are reported. Examples of dielectric analysis on perfluoropolyether microemulsions are given.

1. Introduction

Complex fluids as amphiphile-containing systems exhibit an interfacial dielectric absorption, when submitted to an alternating electric field, which occurs in different frequency ranges depending on the nature of the system. For example, emulsions absorb in the kilohertz range [1, 2], microemulsions in the megahertz range [3–10]. The purpose of this work is to describe a procedure for measuring the dielectric absorption of highly conductive perfluoropolyether microemulsions. A few years ago, some of us found an interesting monophasic region in the ternary phase diagram of perfluoropolyether (PFPE) surfactant, PFPE oil and water [11] of samples having the macroscopic characteristics of microemulsions (transparent, isotropic, stable and low-viscosity fluids). Preliminary analyses pointed out the existence of highly conductive water-in-oil microemulsions: thus conductivity investigation [12, 13], light scattering [14] and nuclear magnetic resonance [15] have been used to characterize the system. We recall the main findings. Aqueous aggregates of size 2–8 nm have been found [12, 14] if at least 4–5 water molecules occur for a surfactant molecule in the compound. The aggregates exhibit strong attractive interactions at low water-to-surfactant (W/S) molar ratio (W/S about 6) whereas the attraction between aggregates decreases with increasing W/S ratio. The onset of droplet-formation (detected by light scattering and NMR), at W/S $\simeq$ 6, corresponds to a conductivity maximum recorded by increasing water along lines of constant O/S ratio (oil-to-surfactant molar ratio), the conductivity maximum increases from 0.05 to 0.35 siemens per metre as the O/S ratio decreases from 5.67 to 1.22. These features suggest investigation of the whole dielectric behaviour of such ternary system throughout the monophasic region of the phase diagram. Furthermore, analysis of the dielectric behaviour at different temperatures is expected to give deeper insight about the interactions between the aggregates of the W/O (water-to-oil molar ratio) PFPE microemulsions. In this paper we describe the use of the impedance analysis technique to detect the complex permittivity and conductivity of PFPE microemulsions up to 100 MHz, with particular regard to the construction of the measuring cells, calibration procedure and numerical analysis. Examples of the dielectric permittivity trend against frequency are reported for the PFPE W/O microemulsions.

2. Experimental

2.1. Experimental equipment

The measurements were performed with a Hewlett Packard 4192A LF impedance analyser in the range 5 Hz to 13 MHz (signal intensity 50 mV to 1 V depending on the sample conductivity) and a Hewlett Packard 4815A RF impedance analyser in the range 5–108 MHz, connected to an external frequency counter HP5382A. The cells (both temperature-controlled) used with these impedance analysers were, respectively, a four- and a

0957-0233/93/050627+05$07.50

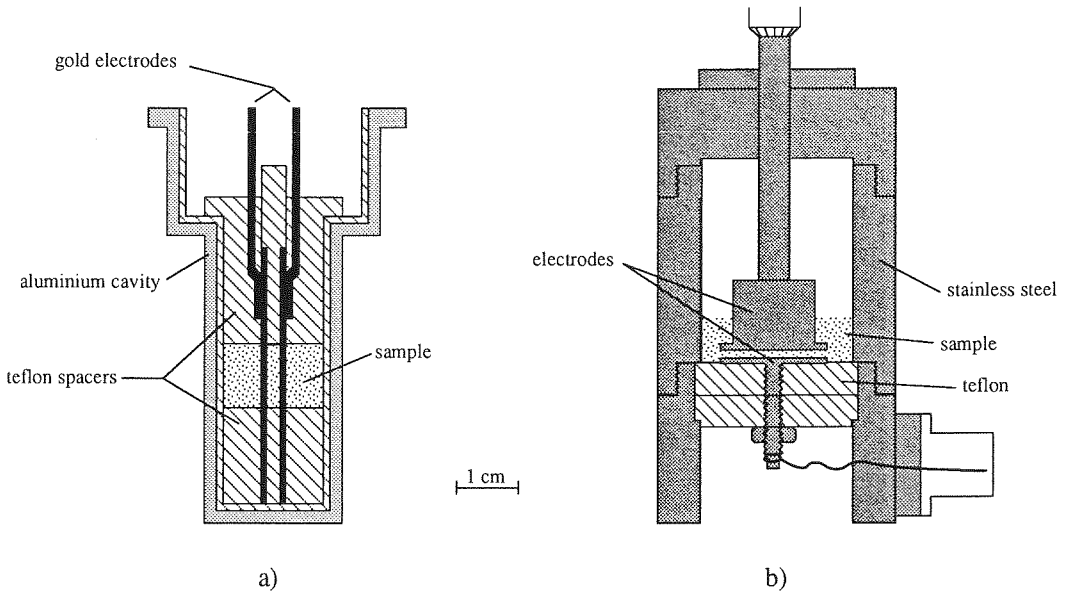

Figure 1. Cell design: (*a*) LF cell; (*b*) RF cell.

two-terminal sample holder device with plane and parallel electrodes (figure 1). The cell used with the LF impedance analyser (figure 1(*a*)) has rectangular gold plate electrodes (dimensions 40 mm × 9 mm × 1 mm) with surfaces roughened to decrease electrode polarization [16] and maintained parallel, at a distance of 3 mm, by Teflon spacers. The cell fits a cylindrical aluminium cavity coated with a Teflon layer of thickness 1 mm and is connected to the LF impedance analyser by the HP 16048A test leads ('four-terminal pair'). The four-terminal configuration is converted to a two-terminal configuration at the cable end by connecting the high and low side cables, respectively, via low-impedance straps to the electrodes in order to minimize parasitic elements; the shields of the four conductors are connected together and to the aluminium cavity. The electrodes and the spacers can be easily disjoined to facilitate cell cleaning. The cell is filled from the top; some care is required to avoid bubble formation. A small hole in the upper spacer closing the cell facilitates air outflow. The measurements are performed at constant volume. Thermal stabilization (±0.1 °C) of the sample is achieved by immersion of the cell in a thermally controlled ethylene glycol bath whose temperature was checked by a mercury thermometer with 0.1 °C resolution. The geometry of the latter cell ensures a reasonably fast variation of temperature; a thermocouple placed inside the cell filled with a sample has demonstrated that a time delay of 10 min is sufficient to obtain thermal stabilization inside the cell, for temperatures in the range −10–60 °C. The cell used with the RF impedance analyser (figure 1(*b*)) has cylindrical stainless steel plate electrodes (dimensions 1.5 mm thickness and 20 mm diameter) with surfaces roughened to decrease the electrode polarization [16]; the distance between the electrodes is 1 mm. The upper electrode is electrically connected to the case of the cell which, in turn, is connected to earth in order to allow volume-independent measurements. The impedance analyser probe is connected to the cell by a probe-to-BNC adapter. A thermally stabilized water flow (±0.1 °C) circulates through a glass jacket containing the cell. Measurement of temperature was by a platinum probe placed on the cell.

Table 1. Parasitic elements and cell constant of the LF and RF cells.

	LF cell	RF cell
C_0(pF)	2.2 ± 0.3	6.80 ± 0.04
L_s(nH)	128.0 ± 0.5	30.6 ± 0.5
R_s(Ω)	0.110 ± 0.007	0.60 ± 0.01
k(10^{-2} m)	4.96 ± 0.03	36.1 ± 0.1

The geometry of the two cells prevents the sample from pressure-induced effects and is suitable for small sample volumes; the construction materials are chemically inert. In the realization of the cells and the electrical connections care was taken to minimize the distributed impedances [17–20] due to reactance contributions and loss effects as well as to extend the lumped element circuit measuring technique up to 100 MHz. Residual parasitic elements (stray capacitance C_0, series inductance L_s and series resistance R_s) have been measured for the LF and RF cells; the values are reported in table 1. The procedure of measuring the parasitic elements and the cell constant is described in section 2.3.

2.2. Determination of the dielectric permittivity

A dielectric material contained between the plates of an ideal parallel-plate capacitor can be represented by an equivalent parallel RC electrical circuit having capacitance

$$C = k\epsilon_0\epsilon' \qquad (1)$$

and conductance

$$G = \omega k \epsilon_0 \epsilon'' + k\sigma \qquad (2)$$

where ϵ_0 is the permittivity of free space, $\epsilon' - j\epsilon''$ is the complex permittivity of the medium ($j^2 = -1$), σ is the frequency-invariant contribution to the conductivity, ω is the angular frequency ($2\pi f$) and k is the cell constant depending only on the cell geometry for such an ideal case. In our case, a stray capacitance (C_0) has to be added in parallel to the previous circuit and a self-inductance (L_s) and a resistance (R_s) have to be added in series. In figure 2 the electrical equivalent circuit is drawn. At each frequency the latter circuit can be described as an RC parallel, say $R_M C_M$; as the experimentally measured quantities are the impedance magnitude $|Z|$ and the phase angle θ, then $R_M = |Z|/\cos\theta$, $C_M = -\sin\theta/\omega|Z|$. Equating the circuit shown in figure 2 to the $R_M C_M$ circuit, the sample resistance $R(= 1/G)$ and the sample capacitance C can be calculated as follows:

$$R = \frac{R_M - R_s b}{b} + \frac{\omega^2 (b L_s + \tau_M R_M)^2}{b(R_M - R_s b)} \qquad (3)$$

$$C = \frac{(bL_s + \tau_M R_M)\, b}{(R_M - R_s b)^2 + \omega^2 (b L_s + \tau_M R_M)^2} - C_0 \qquad (4)$$

where $\tau_M = R_M C_M$ and $b = 1 + \omega^2 \tau_M^2$. We recall that the electrode polarization effect is significant from zero frequency up to a threshold frequency (f_t) which depends on the sample conductivity. In fact the polarization capacitance C_p and the polarization resistance R_p, following Schwan [16], are functions of the frequency according to the relation $C_{p0} f^{-m}$ where C_{p0} and m depend on the sample electrode layer characteristics. Furthermore, as m is positive, both C_p and R_p decrease with a frequency increase; in [16] typical m values are 0.3 for capacitance and 0.5 for resistance. A preliminary analysis of the electrode polarization effect was carried out for each sample studied, in the lowest frequency range. The C_{p0} and m values were estimated. The minimum frequency f_t, above which it is reasonable to exclude the electrode polarization contribution, was established. The m value is about 0.3 for C_p and 0.5 to 0.7 for R_p. The values of R and C for each sample are then obtained by means of R_M and C_M at different frequencies above f_t, through equations (3) and (4). Furthermore, for each sample tested, it is possible to observe a frequency interval over which the sample behaves as a constant resistance R'_M in series with the polarization capacitance, hence the sample conductivity is obtained as $\sigma = (R'_M - R_s)/k$. The values of ϵ' and ϵ'' are then determined from equations (1) and (2).

2.3. Calibration

The following procedure was used to measure the parasitic elements (R_s, L_s, C_0) and the cell constant (k). For the LF cell:

(a) By choosing an aqueous electrolytic solution of proper conductivity, it is possible to measure L_s without knowing the other cell parameters. An aqueous NaCl solution [21] of salinity 25% (salinity is expressed by the weight ratio NaCl/(H_2O+NaCl)) was used and $|Z|$ and θ were measured up to 13 MHz. For such a sample, above f_t (500 KHz), the equivalent circuit of figure 2 reduces to a series of L_s, R_s and R. In fact, $|Z|\sin\theta/\omega$ is constant up to 13 MHz, demonstrating that the capacitance contribution is negligible and that the value of L_s does not vary with frequency. Then L_s is obtained by the relation $L_s = |Z|\sin\theta/\omega$. The average of the L_s measurements in the frequency range 500 kHz–13 MHz is reported in table 1 with its standard deviation. The same study at salinities 10% and 5% confirms the L_s value, in the frequency range 3–13 MHz. At lower ionic content C_p is lower and f_t increases.

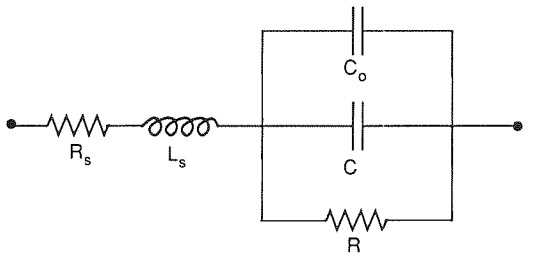

Figure 2. Equivalent network of the cell system: R and C represent the sample resistance and capacitance; R_s, L_s and C_0 are the parasitic elements.

(b) R_s and k have been measured by means of aqueous NaCl solutions with salinity values 0.3%, 0.5%, 1%, 3%, 5%, 10% and 25% [21]. The study of each solution versus frequency (above f_t) suggests that the equivalent circuit is a series of constant self-inductance and resistance, while capacitive contributions are negligible: the resistance value was estimated as an average over measurements at different frequencies for each sample. Thereafter a linear regression analysis of the experimental values of the equation $R_M = R_s + (k\sigma)^{-1}$ was performed to obtain k and R_s. The results and their standard deviations are reported in table 1. The accuracy of the cell geometry has been evaluated independently by repeating the measurements of $|Z|$ and θ five times at different frequencies (for two different solutions), repeating every time the cell-filling procedure. An indeterminacy of ±0.3% was found that was ascribed to the cell constant, the error of k reported in table 1 takes into account the latter contribution.

(c) The capacitance $C + C_0$ of the cell filled with dielectric liquids of known permittivity [22] was obtained from measurements at different frequencies using the equivalent circuit of figure 2. For each liquid the average of the values at different frequencies has been calculated and reported as a function of the dielectric permittivity ϵ' of the sample (liquids used were cyclohexane, t-butyl acetate, 1,2-dichloroethane, glycerol and water). A linear regression analysis of the experimental data to equation (1) determines k and C_0. C_0 and its standard deviation are reported in table 1, the new value of k confirms the value obtained in (b).

For the RF cell:

(d) L_s was measured, filling the cell with dielec-

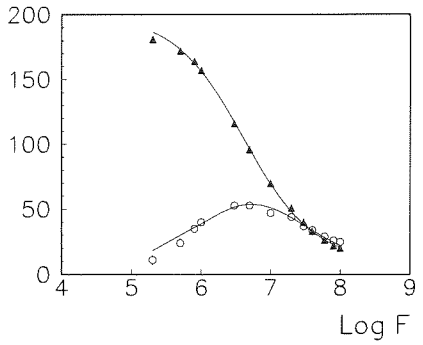

Figure 3. Measured and calculated complex permittivity versus frequency (F is frequency in hertz) for a PFPE W/O microemulsion with W/S = 0.3 w/w and O/S = 1.71 w/w. Triangles: ϵ'; circles: ϵ''.

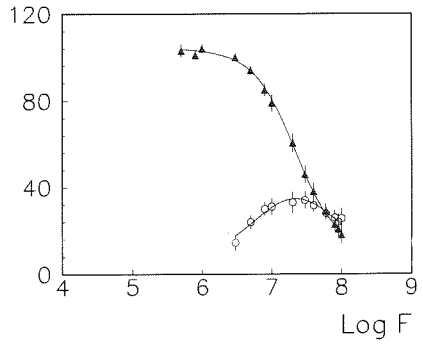

Figure 4. Measured and calculated complex permittivity versus frequency (F is frequency in hertz) for a PFPE W/O microemulsion with W/S = 0.3 w/w and O/S = 0.87 w/w. Triangles: ϵ'; circles: ϵ''.

tric liquids whose permittivity was known and constant over the frequency range of the apparatus [22] (liquids used were methanol, nitrobenzene, dimethyl sulphoxide and water). The electrical circuit reduces to a series of R_s, L_s and $C + C_0$, as R is very large. Furthermore electrode polarization is always negligible. Using this simplified circuit, it follows that $\omega|Z|\sin\theta = -\omega^2 L_s + 1/(C + C_0)$. The plot of $\omega|Z|\sin\theta$ against ω^2 shows a linear relationship for all the dielectric liquids used over the whole frequency range of the RF impedance analyser, demonstrating that L_s does not vary with frequency. The L_s value was obtained by linear regression of the experimental points for each dielectric liquid and averaged over the several liquids (results in table 1). The procedure reported in (a) for the LF cell is less satisfactory in this case; aqueous NaCl solutions with salinities 5% and 10% have been investigated; electrode polarization affects the results up to 20 MHz. The value found is less accurate, though consistent with that of table 1.

(e) R_s, C_0 and k have been determined as for the LF cell. Their values and standard deviations are reported in table 1. The accuracy of the cell geometry is ±0.3%, as for the LF cell, and the error of k takes into account this contribution.

Chemical fluids used for calibration were NaCl and methanol from Merck (analytical grade), nitrobenzene and t-butyl acetate from Merck (by synthesis), dimethyl sulphoxide from Sigma (reagent grade), cyclohexane from Hoechst-Riedel de Haen (spectranalar), 1,2-dichloroethane from Merck (uvasol), glycerol from BDH (analar). Water is taken from a Milli-Q water system (Millipore).

Table 2. Dielectric permittivity, relaxation time and spread parameter of the PFPE microemulsion samples A (figure 3) and B (figure 4).

	A	B
ϵ_l	202 ± 4	104 ± 2
ϵ_h	6 ± 3	10 ± 6
τ_s(ns)	39 ± 2	7 ± 1
α	0.64 ± 0.02	0.87 ± 0.05

3. Results

Examples of measurements of the dielectric permittivity versus frequency of the PFPE W/O microemulsions are shown in figures 3 and 4. The samples are microemulsions of the ternary phase diagram [11], belonging to the straight line W/S=0.3 w/w (weight by weight); the O/S ratio is 1.71 w/w for the sample of figure 3 (sample A) and 0.87 w/w for the sample of figure 4 (sample B). The sample conductivity (σ) and its standard deviation are $(28.0 \pm 0.2) \times 10^{-3}$ siemens per metre for sample A and $(137 \pm 1) \times 10^{-3}$ siemens per metre for sample B. ϵ' and ϵ'' have been obtained for each frequency from relations (1) and (2) above. The error bars (standard deviation) are drawn except when they are smaller than the symbol used. The error of the frequency measurement (less than ±50 ppm) is negligible. The trend of ϵ' and ϵ'' versus frequency is typical of the dielectric absorption due to interfacial polarization (or Maxwell–Wagner polarization) and the frequency range of the absorption is typical of microemulsion systems [3–10]. The continuous lines of figures 3 and 4 represent the functions $\epsilon'(f)$ and $\epsilon''(f)$ [1, 10]:

$$\epsilon' - j\epsilon'' = \epsilon_h + \frac{\epsilon_l - \epsilon_h}{1 + (j\omega\tau_s)^\alpha} \qquad (6)$$

as obtained by the fit program Minuit [23]. In the latter equation ϵ_l is the real part of the dielectric permittivity extrapolated at zero frequency (static permittivity of the sample), ϵ_h is the plateau high frequency value of ϵ', τ_s is the relaxation time and α is the spread parameter [1, 10]. Results of the fitting procedure with their standard deviations are shown in table 2.

Acknowledgments

This work was partially supported by Ausimont SPA and by MURST 40% and 60% funds. MGG thanks Ausimont for having supported her during this research work. The authors wish to express their appreciation to the referees for their very helpful criticisms.

References

[1] Clausse M 1983 Dielectric properties of emulsions and related systems *Encyclopedia of Emulsion Technology* vol 1, ed P Becher (New York: Marcel Dekker) pp 481–715

[2] Hanai T, Imakita T and Koizumi N 1982 Analysis of dielectric relaxations of w/o emulsions in the light of theories of interfacial polarization *Colloid Polym. Sci.* **260** 1029–34

[3] Clausse M, Sheppard R J, Boned C and Essex C G 1976 Dielectric study of water-in-hexadecane microemulsions. A preliminary report *Colloid and Interface Science* vol II, ed M Kerker (New York: Academic) pp 233–43

[4] Senatra D and Giubilaro G 1978 Dielectric study. I. Critical phenomena behavior in phase transition of water-in-oil microemulsions. II Structural transitions in the liquid crystalline phase of water-in-oil microemulsions *J. Colloid. Interface Sci.* **67** 448–56; 457–64

[5] Senatra D, Guarini G G T and Gabrielli G 1985 Interfacial polarization, pyroelectricity and heat content in w/o microemulsions *Physics of Amphiphiles: Micelles, Vescicles and Microemulsions* (Bologna: Societá Italiana di Fisica) pp 802–29

[6] Senatra D, Gabrielli G, Caminati G and Zhou Z 1988 Conformational Changes at the microemulsion water/ oil interface and their influence on the system's dielectric temperature behavior *IEEE Trans. Electr. Insulation* **23** 579–89

[7] Peyrelasse J and Boned C 1985 Study of the structure of water/aerosol OT/dodecane systems by time domain dielectric spectroscopy *J. Phys. Chem.* **89** 370–9

[8] Van Dijk M A, Broekman E, Joosten J G H and Bedeaux D 1986 Dielectric study of temperature dependent aerosol OT/water/isooctane microemulsion structure *J. Physique* **47** 727–31

[9] Hodge I M and Angell C A 1978 The relative permittivity of supercooled water *J. Chem. Phys.* **68** 1363–8

[10] Chou S I and Shah D O 1981 *J. Phys. Chem.* **85** 1480–5

[11] Chittofrati A, Lenti D, Sanguineti A, Visca M, Gambi C M C, Senatra D and Zhou Z 1989 Perfluoropolyether microemulsions *Progr. Colloid. Polym. Sci.* **79** 218–25

[12] Chittofrati A, Sanguineti A, Visca M and Kallay N 1992 Perfluoropolyether microemulsions: conductivity behaviour of three component w/o systems *Colloid. Surf.* **63** 219–33

[13] Chittofrati A, Visca M and Kallay N 1993 Perfluoropolyether microemulsions: conductivity behaviour of four-component W/O systems *Colloid. Surf.* at press

[14] Sanguineti A, Chittofrati A, Lenti D and Visca M 1993 Light scattering study of a perfluoropolyether ternary system *J. Colloid. Interface Sci.* **155**

[15] Monduzzi M, Chittofrati A and Visca M 1992 Perfluoropolyether W/O microemulsions: a ^{1}H NMR self-diffusion study of water *Langmuir* **8** 1278–84

[16] Schwan H P 1963 Determination of biological impedances *Physical Techniques in Biological Research* vol VI(B), ed W L Nastuk (New York: Academic) pp 323–406

[17] O' Konski C T and Edwards A 1968 Cell for dielectric measurements in the high radio frequency region *Rev. Sci. Instrum.* **39** 1456–8

[18] Jordan B P and Grant E H 1970 A cell for measuring the complex permittivity of lossy liquids at very high radio frequencies *J. Phys. E: Sci. Instrum.* **3** 764–6

[19] Essex C G, South G P, Sheppard R J and Grant E H 1975 A bridge technique for measuring the permittivity of a biological solution between 1 and 100 MHz *J. Phys. E: Sci. Instrum.* **8** 385–9

[20] Asami K, Irimajiri A, Hanai T and Koizumi N 1973 A method for estimating residual inductance in high frequency a.c. measurements *Bull. Inst. Chem. Res. Kyoto Univ.* **51** 231–45

[21] *CRC Handbook of Chemistry and Physics* 70th edn 1989–1990 (Boca Raton, Florida: CRC)

[22] Maryott A A and Smith E R 1951 Table of dielectric constants of pure liquids, NBS circular 514, United States Department of Commerce, National Bureau of Standards, USA

[23] James F 1972 Function minimization *Proc. 1972 CERN Computing and Data Processing School, Partisau, Austria, 10–24 September* (CERN 72-21)